Relation between Intrinsic Hydrogen and AE Sources in Elastic Region during Tensile Deformation of Al-Mg-Si Alloys

K. YOSHIDA, Y. TOKUYAMA and T. KUBO
Faculty of Science and Engineering, Tokushima Bunri University
1314-1 Shido, Sanuki City, Kagawa 769-2193, Japan
kenyoshida@fst.bunri-u.ac.jp

Abstract. Acoustic emission (AE) behavior during tensile deformation of Al-Mg-Si alloy has been investigated. We prepared some kinds of the Al-Mg-Si alloy with three different chemical compositions, consisting of magnesium and silicon balanced, excess silicon and excess copper alloys. As for the heat treatment, the specimens were solution-treated at 540℃ for 1 hour, aged at 175℃ for 30 minutes and finally aged at room temperature for 7 days (T4 treatment). The two cooling rates of water quenching and air-cooling after solution treatment were selected. As a result, the tensile property and AE behavior were changed with the change of the cooling rate. From SEM observation, the fracture surface by the air-cooling after the solution treatment was covered with intergranular fracture because the ductility decline. The AE events of the air-cooling specimens during tensile deformation were detected in the elastic region. The source rise time was analyzed using the S0 mode Lamb waveform of the AE, and appearances were also observed using the specimen also SEM, TEM and optical microscope.

In this paper, we focused on and estimated the AE sources observed during the elastic deformation. It was clear that the AE source was the micro- intergranular fracture depending upon the precipitates in the grain boundary of the copper excess specimen air-cooled and the micro-intergranular fracture had no progress to the final failure. It was considered that the micro-intergranular fracture depended upon the hydrogen trapped at the triangle junction of the grain boundaries and along the precipitates in the grain boundaries, and after that the hydrogen was emitted during the elastic deformation. Finally, in order to confirm the effect of the hydrogen behavior on the AE activity whether it is trapped easily or nots, a tensile test of Al-Mg-Si alloy has been conducted using a notched specimen hydrogen-charged in a sodium hydroxide solution. As a result, it was clear that the hydrogen was trapped easily at the short time but easy to eject.

1. Introduction

Recently the weight of the car is lightening for CO_2 reduction as one of the global warming countermeasures. The Al-Mg-Si alloy (6000 series) is applied to automotive body panels to increase a mileage. This alloy is one of the heat-treatable aluminum alloys. The heat-treated aluminum alloy is strengthened by intended secondary-phase particles precipitated when heat treatments such as solution treatment, quenching and aging, were properly performed. However, it is reported that the intergranular fracture is easy to generate when the cooling

rate after the solution treatment is low because of thick and large materials [1]. In fact, we have confirmed in the past study [2] that the intergranular fracture was generated due to air-cooling process after solution treatment in the Al-Mg-Si alloy with Cu additive and the characteristic acoustic emission (AE) behavior could be observed during the tensile deformation, especially in the elastic region. The AE events in the specimens due to water-quenching process after the solution treatment could not be observed in the elastic region but observed during the yielding.

In this paper, we focused on and estimated the AE sources observed during the elastic deformation. It was clear that the AE source was the micro-intergranular fracture depending upon the precipitates in the grain boundary of the copper excess specimen air-cooled and the micro-intergranular fracture had no progress to the final failure. It was considered that the micro-intergranular fracture depended upon the hydrogen trapped at the triangle junction of the grain boundaries and along the precipitates in the grain boundaries, and after that the hydrogen was evolved during the elastic deformation. Finally, in order to confirm the effect of the hydrogen behavior on the AE activity whether it is trapped easily or not, a tensile test of Al-Mg-Si alloy with magnesium and silicon balanced has been conducted using a notched specimen hydrogen-charged in a sodium hydroxide solution.

2. Experimental Procedure

2.1 Specimen and heat treatment

Three types of specimens with different chemical compositions (A3, A4 and A8) were used in this study. The chemical compositions of these specimens are shown in Table 1. SpecimenA3 is with Mg and Si additives balanced for Mg_2Si precipitate forming, specimen A4 is with excess Si additive, and specimen A8 is with balanced and Cu additives. These specimens for tensile test were prepared using an electrical discharge machine (Brother HS-300). The shape of the specimens for tensile test are shown in Fig.1 (a) and (b). The smooth specimens in Fig.1(a) were prepared for the tensile test of specimen A3, A4 and A8. The notched specimen in Fig.1(b) was prepared for the tensile test of the air-cooled and hydrogen-charged specimen A3. The tensile direction was vertical to the rolling direction of the Al-Mg-Si alloy plates.

Table.1 Chemical composition of specimens (mass%)

	Mg	Si	Cu	Fe	Mn	Zn	Al
A3	0.97	0.56	<0.01	<0.03	<0.01	<0.01	Bal.
A4	0.70	0.87	<0.01	<0.03	<0.01	<0.01	Bal.
A8	0.95	0.55	0.34	<0.03	<0.01	<0.01	Bal.

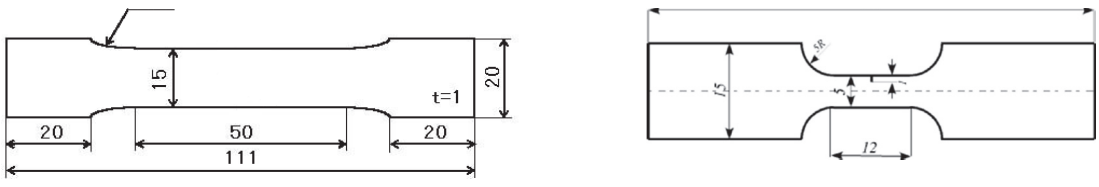

(a) smooth specimen (b) notched specimen for hydrogen-charging

Fig.1 Shape of specimens for tensile test (mm)

The specimens were solution-treated at 540℃ for 1 hour, air-cooled and water-quenched after the solution treatment, naturally aged for 7 days and aged at 175℃ for 30 min (Bake hard treatment).

The notched specimen was hydrogen-charged by soaking in 0.1N sodium hydroxide solution for 0s, 10s and 30s, respectively. The chemical reaction is as follows[3] : $2Al + 2NaOH + 6H_2O \rightarrow 2Na[Al(OH)_4] + 3H_2$

2.2 Tensile test and AE measurement

Tensile test was carried out using Instron-type machine (Shimadzu Autograph) at strain rate of 6.7×10^{-6} s^{-1} at ambient temperature.

We attached two AE sensors (Fuji Ceramics M5W) separated by 70 mm in the smooth specimen and 30 mm in the notched specimen from the center of the specimen, respectively. AE measurement was made using 2-channnel AE monitoring system to discriminate the grip noise. The threshold level was 40dB. The AE during the tensile test was transformed into the electrical signal by AE sensors, and then the signal was amplified by a constant gain of 40dB and passed through a band-pass filter of 100Hz to 20MHz (NF 9913). Finally AE waveforms were sent to the digital multi-recorder (Keyence GR-7000) in which the sampling time was 50ns, and were analysed off-line.

2.3 Optical, SEM and TEM observations

Surface appearance was observed after corroded in the solution with distilled water of 166ml, nitric acid of 20ml and hydrogen fluoride of 14ml using a digital optical microscope (Keyence VHX-600). Fracture surface was observed and qualitative EDX analysis was conducted using FE-SEM (Hitachi S-4700). Observation of precipitates and dislocations was conducted using TEM (Hitachi H-800) after a twin jet electro-polishing at -12.0℃ on 10.5V in the solution with perchloric acid of 100ml, glycerin of 200ml and methyl alcohol of 700ml.

3. Results and Discussion

3.1 Tensile properties and fracture appearances

The tensile properties of each specimen are shown in Fig.2. It was shown that the yield strength and the tensile strength of specimens air-cooled after the solution treatment were

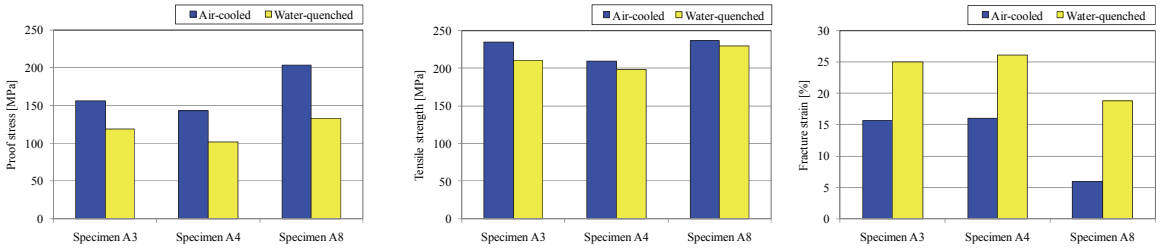

(a) Yield strength (b) Tensile strength (c) Fracture strain

Fig. 2 Tensile properties, consisting of (a) yield strength, (b) tensile strength and (c) fracture strain, in specimen A3, A4 and A8 air-cooled and water-quenched

higher than those water-quenched. Especially the yield strength air-cooled was higher 43MPa in specimen A3, 32MPa in specimen A4 and 59MPa in specimen A8 than those water-quenched, respectively. The yield strength and the tensile strength in specimen A8 with excess Cu additive were much higher than those in the other. It was considered that the age hardening increased with Cu additive [4]. In contrast, the fracture strains in the specimens air-cooled were lower about 9% in specimen A3, about 13.5% in specimen A4

and about 12.7% in specimen A8 than those water-quenched, respectively. It was confirmed that the three specimens air-cooled showed very low ductility compared with those water-quenched, especially the lowest ductility in specimen A8 air-cooled because of the excess Cu additive.

The fracture surface water-quenched was covered with large and deep transgranular dimples. The secondary-phase particles were not observed at the bottom of the transgranular dimples. On the other hand, the fracture surface air-cooled was covered with intergranular fracture and the surface consisted of small and shallow intergranular dimples. A lot of secondary-phase particles in the size of about 0.5μm were observed at the bottom of the intergranular dimples as shown in Fig. 3. The fracture surfaces in specimens A3 and A4 water-quenched and air-cooled showed the similar aspect in specimen A8, respectively.

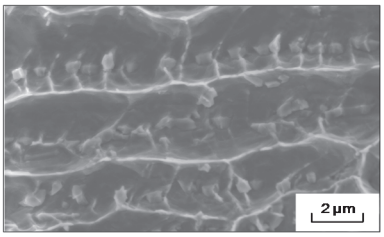

Fig. 3 Typical example of intergranular fracture in the specimen A8 air-cooled

The typical grain boundary precipitation can be seen in the air-cooled specimens, although there is no precipitation along the grain boundary in the water-quenched specimens.

These results were summarized as follows. A large number of secondary-phase particles including Al, Mg, Si and Cu elements were precipitated during air-cooling. Because the secondary-phase particles work as precipitate strengthening, the proof stress and the tensile strength show higher values. However, these precipitates generated along the grain boundaries lead easily to the intergranular cracking. As a result, the fracture surface in the specimens air-cooled is covered with small and shallow dimples.

3.2 AE activities during tensile test

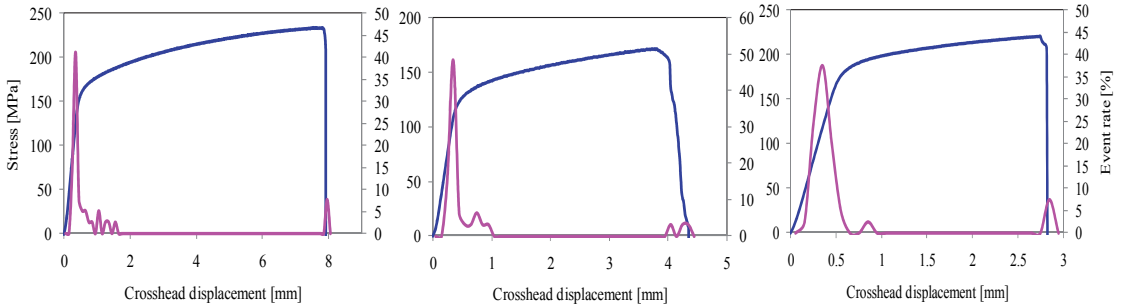

(a) Specimen A3 (29) (b) Specimen A4 (31) (c) Specimen A8 (40)

Fig. 4 AE event rates during tensile test in specimen A3, A4 and A8 air-cooled with the stress-displacement curves. The number in the bracket shows the total event count.

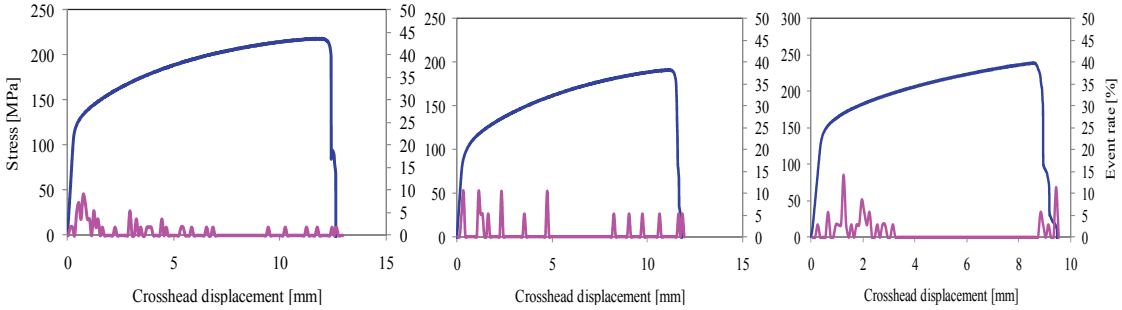

(a) Specimen A3 (55) (b) Specimen A4 (16) (c) Specimen A8 (36)

Fig. 5 AE event rates during tensile test in specimen A3, A4 and A8 water-quenched with the stress-displacement curves. The number in the bracket shows the total event count.

The AE event rates during tensile test in specimen A3, A4 and A8 air-cooled and water-quenched are shown with the stress-displacement curves in Fig. 4 and 5, respectively. The proportion of the event count detected at the displacement of 0.1 mm intervals to the total event count. The event rate in the air-cooled specimens is detected in the elastic region xand around yield point in Fig. 4. The peak event rates in the elastic region that occupy the values of 40% to 50% shows the very high level compared to the peak rate around yield point. The AE event rate behavior in the elastic region was same in the air-cooled specimens regardless of the sort of the additive element. On the other hand, the event rate around yield point in the water-quenched specimens almost shows the peak rate of 10% to 15% in Fig. 5. The AE source at the peak of the event rate is considered to be due to the collective motion of dislocations. The event rate in all water-quenched specimens decreases with the deformation in progress, which is explained by decrease of mean free path of dislocations [5].

3.3 Source specification of AE events detected in the elastic region

Several experiments have been conducted to specify the source of AE events detected in the elastic region during tensile deformation in the air-cooled specimens.

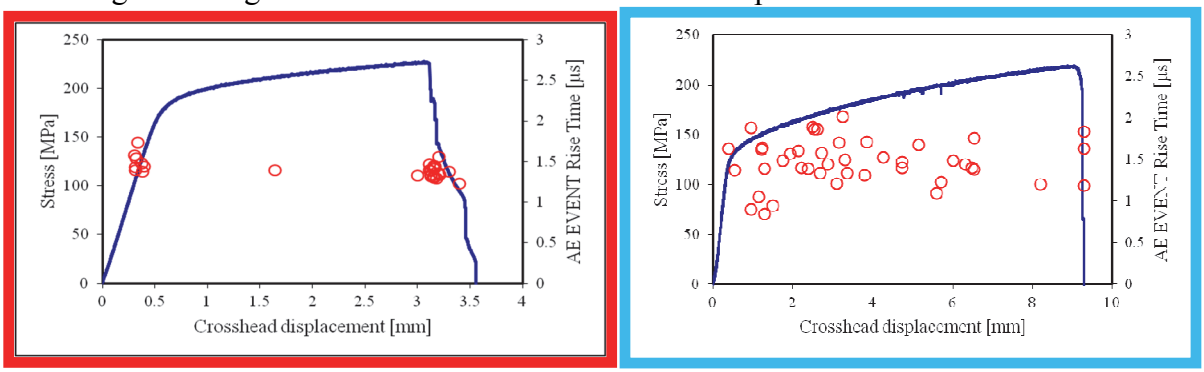

(a) Specimen A8 air-cooled (b) Specimen A8 water-quenched

Fig. 6 Relationship between the source rise times analyzed by AE waveform detected in specimen A8 (a) air-cooled and (b) water-quenched with the stress-displacement curves

We tried to introduce the AE source rise time to characterize the AE source in the elastic region. The AE source rise time was analyzed using the estimation method proposed by T. Yasuda et al. [6] that was obtained using the AE waveform detected during martensitic transformation of Cu-Al-Ni shape memory alloy single crystal. The source rise time represents the rise time of the step function in the AE source. The relationship between the source rise times analyzed by AE waveform detected in specimen A8 air-cooled and water-quenched is shown with the stress-displacement curves in Fig. 6. The source rise time in the air-cooled is concentrated on 1.2～1.7μs in Fig. 6(a) but in the water-quenched is dispersed in Fig. 6(b). The source rise time in the elastic region of the air-cooled is same as that in the final failure as shown in Fig. 6(a), so it is possible for the AE source in the elastic region to be the intergranular fracture because of the predominantly intergranular fracture in the final failure as mentioned previously. It is clear that the collective motion of dislocations have the extended source rise time in Fig. 6(b).

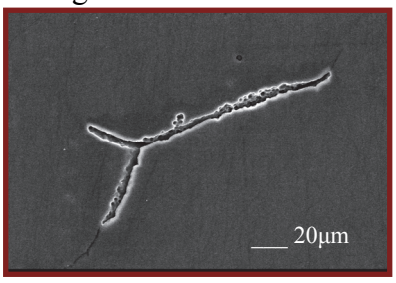

Fig. 7 Surface appearance after the peak event rate in the elastic region.

The surface appearance after the peak event rate in the elastic region is shown in Fig. 7. We can find out the micro-intergranular fracture in the several parts of the surface. This agrees with the result of the source rise time and is considered to be one of the important evidences for the AE source in the elastic region.

3.4 Hydrogen behavior in the Al-Mg-Si alloys

It is reported [3,7] that hydrogen is one of the impurities to badly influence almost mechanical properties in Al alloys. However, it is difficult to understand the hydrogen behavior because it is the smallest atom. Recently the behavior is becoming clear using analytical methods peculiar to hydrogen.

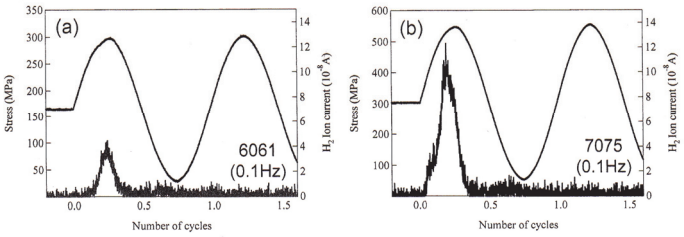

Fig. 8 Hydrogen evolution during the cyclic deformation tested at a frequency of 0.1 Hz. (a) 6061 and (b) 7075 Al alloys by K. Horikawa et al.

There is the hydrogen enhanced local plasticity (HELP) theory by H. K. Birmbaum et al [8] that dislocations are easy to move due to the existence of hydrogen. Here is a result by K. Horikawa et al [9] as shown in Fig. 8 that the hydrogen evolution was only admitted at the first one cycle of cyclic deformation in (a) 6061 and (b) 7075 Al alloys. Finally the relation between stress-displacement curves and AE event rate during tensile test of the notched specimen A3 air-cooled as a function of the soaking time of (a) 0 s., (b) 10 s. and (c) 30 s. are shown in Fig. 9. The tensile test was conducted right away after the soaking. The AE event rate does not increase with increase of the soaking time, that is, the charged hydrogen. Therefore, it is clear that the dynamic behavior of hydrogen is complicated.

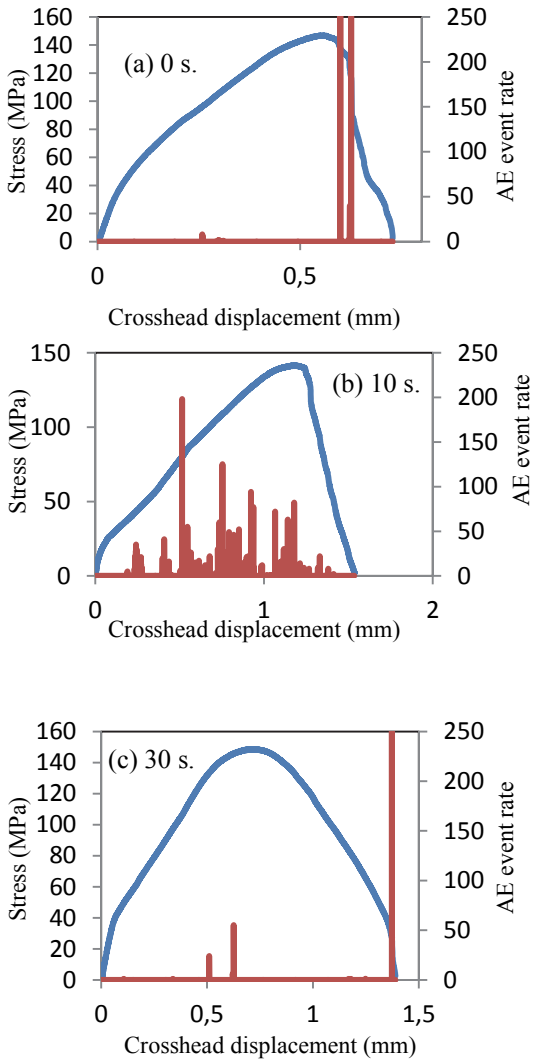

Fig. 9 Relation between stress-displacement curves and AE event rate during tensile test of the notched specimen A3 air-cooled as a function of the soaking time of (a) 0 s., (b) 10 s. and (c) 30 s. in the 0.1N Na(OH) solution.

To discuss the AE activity in the elastic region, it was considered that the micro-intergranular fracture depended upon the hydrogen trapped at the triangle junction of the grain boundaries and along the precipitates in the grain boundaries, where the moving dislocations piled up during the elastic deformation of Al-Mg-Si alloys air-cooled, and after that the hydrogen was evolved during the elastic deformation because the mico-intergranular fracture had no progress to the final failure.

4. Conclusions

The change of the mechanical properties and AE activities in the specimens air-cooled and water-quenched after the solution treatment has been examined during tensile test of Al-Mg-Si alloys with different additives. Especially, the experiment has been conducted in detail to specify the generation of the AE event in the elastic region and the AE source. The results obtained are as follows.

(1) The air-cooled specimen showed higher proof stress, tensile strength and lower ductility than the water-quenched one, which led to the intergranular fracture due to the precipitates segregated along the grain boundaries.
(2) In the case of the air-cooled specimens, the peak AE event rates were shown in the elastic region.
(3) The AE source rise time near the peak of the event rate agreed with that in the final failure.
(4) From the surface appearance observation after the peak event rate, the several mico-intergranular fractures could be found in specimen A8 air-cooled with Cu additive.
(5) As a result, the AE source in the elastic region was considered to be micro-intergranular fracture. It is considered that the fracture depend upon the hydrogen behavior evolved during the elastic deformation.

References

[1] T. Sakurai, K. Matsumoto, S. Komatsu and N. Kono: Journal of Japan Institute of Light Metals, Vol. 60, No. 1, pp. 2-6, 2010.
[2] Y. Kuniyasu, Y. Tokuyama, H. Nishino and K. Yoshida: Progress in Acoustic Emission XV, Vol. 20, pp. 55-60, 2010.
[3] T. Ohnishi: Journal of Japan Institute of Light Metals, Vol. 49, No. 6, pp. 235-251, 1989.
[4] H. Suzuki, M. Kanno, Y. Shiraishi and K. Hanawa: Journal of Japan Institute of Light Metals, Vol. 29, No. 12, pp. 575-581, 1979.
[5] J. Masuda: J. Japan Inst. Metals. Vol. 45, No. 10, pp. 1086-1093, 1981.
[6] T. Yasuda, B. Pang, H. Nishino and K. Yoshida: Materials Transactions, Vol. 52, No.3, pp. 397-405, 2011.
[7] G. Itoh: Journal of Japan Institute of Light Metals, Vol. 63, No. 2, pp. 79-90, 2013.
[8] H. K. Birmbaum and P. Sofronis: Mater. Sci. Eng., A, 176, pp.191-202, 1994.
[9] K. Horikawa, H. Yamada and H. Kobayashi: Journal of Japan Institute of Light Metals, Vol. 62, No. 8, pp. 306-312, 2012.